DETECTION OF A TRANSIENT X-RAY ABSORPTION LINE INTRINSIC TO THE BL LACERTAE OBJECT H 2356-309

Taotao Fang[1], David A. Buote[1], Philip J. Humphrey[1], Claude R. Canizares[2]
(Received; Revised; Accepted)
Draft version February 18, 2011

ABSTRACT

Since the launch of the *Einstein* X-ray Observatory in the 1970s, a number of broad absorption features have been reported in the X-ray spectra of BL Lac objects. These features are often interpreted as arising from high velocity outflows intrinsic to the BL Lac object, therefore providing important information about the inner environment around the central engine. However, such absorption features have not been observed more recently with high-resolution X-ray telescopes such as *Chandra* and *XMM*-Newton. In this paper, we report the detection of a transient X-ray absorption feature intrinsic to the BL Lac object H 2356-309 with the *Chandra* X-ray Telescope. This BL Lac object was observed during *XMM* cycle 7, *Chandra* cycle 8 and 10, as part of our campaign to investigate X-ray absorption produced by the warm-hot intergalactic medium (WHIM) residing in the foreground large scale superstructure. During one of the 80 ksec, *Chandra* cycle 10 observations, a transient absorption feature was detected at 3.3σ (or 99.9% confidence level, accounting for the number of trials), which we identify as the O VIII Kα line produced by an absorber intrinsic to the BL Lac object. None of the other 11 observations showed this line. We constrain the ionization parameter ($25 \lesssim \Xi \lesssim 40$) and temperature ($10^5 < T < 2.5 \times 10^7$ K) of the absorber. This absorber is likely produced by an outflow with a velocity up to $1,500$ km s^{-1}. There is a suggestion of possible excess emission on the long-wavelength side of the absorption line; however, the derived properties of the emission material are very different from those of the absorption material, implying it is unlikely a typical P Cygni-type profile.

Subject headings: BL Lacertae objects: individual (H 2356-309) — quasars: absorption lines

1. INTRODUCTION

Blazars, characterized by their highly polarized emission in the optical band and strong variability at almost all frequencies, are often interpreted as active galactic nuclei (AGNs) with relativistic jets beamed toward us (see, e.g., Angel & Stockman 1980). BL Lac objects, which are a sub-class of blazars, typically exhibit weak or no spectral features in emission or absorption at all wavelengths (e.g., Urry & Padovani 1995). In particular, the very few weak absorption features detected in the optical band are believed to originate in the interstellar medium of the host galaxy (e.g., see Sbarufatti et al. 2005; Plotkin et al. 2010) and have been used to determine the redshift of the BL Lac object. Therefore, unlike the typical warm absorbers seen in AGNs, optical absorption lines in BL Lac objects offer no information about the immediate environment of the central black holes.

However, in the X-ray band, Canizares & Kruper (1984) reported the first detection of an absorption feature in the spectrum of the BL Lac object PKS 2155-304, using the objective grating spectrometer on the *Einstein Observatory*. Since then a number of X-ray absorption features have been reported (see, e.g., Urry et al. 1986; Madejski et al. 1991; Grandi et al. 1997; Sambruna et al. 1997), leading to the conclusion that such X-ray ab-

sorption features are quite common in the spectra of BL Lac objects. These features were typically broad (with a width of a few tens of eV up to a few hundred eV) in the soft X-ray band, and were often interpreted as resonant absorption from highly ionized oxygen originating in a high velocity outflow (up to a few 10,000 km s^{-1}) intrinsic to the BL Lac object (e.g., Krolik et al. 1985). These discoveries demonstrate that X-ray absorption features can provide an extremely valuable probe of the central region of BL Lac objects.

Since the launch of the *Chandra* and *XMM*-Newton X-ray telescopes, a number of BL Lac objects have been observed with unprecedented high spectral resolution. However, so far no *intrinsic* X-ray absorption lines have been detected. *Non-intrinsic* X-ray absorption features have been reported in these BL Lac observations. But unlike previously detected features, when observed with high-resolution these features are typically narrower (width of a few eV or less) and often attributed to the foreground Galactic (e.g., Nicastro et al. 2002; Fang et al. 2003; Rasmussen et al. 2003) or intergalactic origins (e.g., Fang et al. 2002; Nicastro et al. 2005; Buote et al. 2009 – B09 hereafter; Fang et al. 2010 – F10 hereafter). Blustin et al. (2004) and Perlman et al. (2005) examined a number of bright BL Lac objects with *XMM*-Newton. They did not detect any broad features and argued the previous detections were affected by poor spectral quality, calibration uncertainties, as well as the simplification of the continuum model. Although in Blustin et al. (2004) they found a few highly significant features (more than expected from statistic fluctuations), they were not able to find plausible identification of them, casting doubt on

[1] Department of Physics & Astronomy, 4129 Frederick Reines Hall , University of California, Irvine, CA 92697; fangt@uci.edu
[2] Department of Physics and Kavli Institute for Astrophysics and Space Research, Massachusetts Institute of Technology, Cambridge, MA 02139
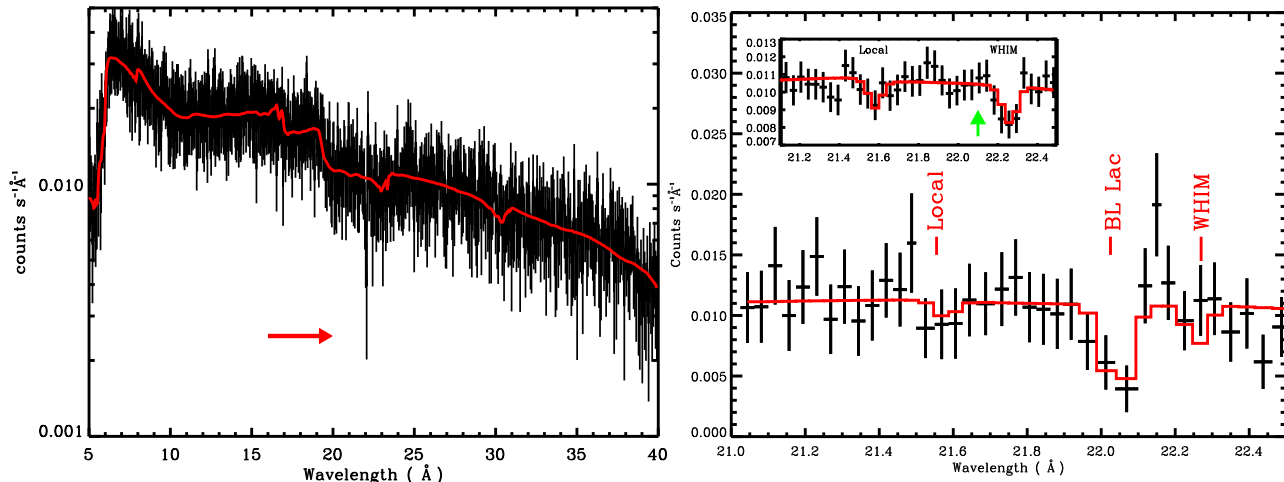
FIG. 1.— The X-ray spectrum of H 2356-309, taken from the observation #10498, plotted in the observer's frame. Left panel shows the entire spectrum between 1 and 40 Å. The red line is a simple fit with a power law and the Galactic absorption. The 22.05 Å feature (indicated by a red arrow) is clearly visible. Right panel shows the spectrum between 21 and 22.5 Å. Red line is the model with three absorption features, one at 21.6 Å (local Galactic O VII K_α absorption), one at 22.05 Å (O VIII K_α absorption intrinsic to the BL Lac), and one at 22.3 Å(redshifted O VII K_α absorption associated with the WHIM in the Sculptor Wall). We fixed the Galactic and WHIM lines at the values measured in F10. Also shown in the inset is the stacked spectrum of H 2356-509 from the other ten Chandra observations (see F10). The two red absorption lines are the local and the Sculptor Wall (WHIM) O VII K_α lines (see F10). The green arrow indicates the wavelength of the transient feature seen in the observation #10498.

the existence of any absorption lines intrinsic to BL Lac objects.

In this paper, we report the serendipitous detection of a transient absorption feature during our multiple observations of the BL Lac object H 2356-309 with gratings on board the *Chandra* and *XMM*-Newton X-ray telescopes. The primary science goal was to study the narrow absorption features produced by the warm-hot intergalactic medium (WHIM) along the sight line toward the BL Lac object. We clearly detected an O VII absorption line produced by the WHIM in the Sculptor Wall, a superstructure along the sight line at $z \sim 0.03$ (B09, F10). During one of the exposures (observation #10498), a strong absorption feature was identified at ~ 22.05 Å. None of the other 11 *Chandra* and *XMM*-Newton observations showed this feature. In this paper we discuss several possibilities of the origin of this transient feature, and conclude it is unlikely an instrumental feature. The most likely explanation is an intrinsic, transient feature produced by hydrogen-like oxygen. We also discuss the constraints on the temperature and ionization structure.

2. DATA ANALYSIS

H 2356-309 is a BL Lac object located at $z = 0.165 \pm 0.002$ (Falomo 1991). Multi-wavelength observations of this target showed its broad-band spectrum can be well described by the synchrotron self-Compton emission from the relativistic jet (e.g., HESS Collaboration et al. 2010). Its sight line passes through a large-scale superstructure of galaxies, the Sculptor Wall, at $z \sim 0.03$ (see Figure 1 of B09). With *XMM*-Newton it was observed in 2007 for approximately 130 ksec (ObsID 0504370701; see B09). With *Chandra* it was observed first in 2007 during cycle 8 for 100 ksec, and then again in 2008 during cycle 10 in ten separate exposures totaling 500 ksec. The *Chandra* exposures range from ~ 15 to 100 ksec (see Table 1 of F10).

Observation #10498 was performed on September 22nd, 2008, for 80 ksec. As in B09 and F10, we followed the standard procedures to extract the spectra. We used the software package CIAO (Version 4.0[3]) and calibration database CALDB (Version 3.5[4]) developed by the *Chandra* X-ray Center. We refer readers to B09 and F10 for details of data extraction, and only want to emphasize a few issues here. First, we have generated our own type II pha file, rather than using the file produced by the standard pipeline (Reprocessing III), to take advantage of an improved background filter not yet available in the standard processing (Wargelin et al. 2009)[5]. Secondly, to account for the high-order contributions of the LETG-HRC, we built a combined response matrix to include the first to the sixth-order contributions (see B09 and F10 for details). Finally, we rebinned the spectrum so that we have at least 40 counts per bin to enhance the spectral signal-to-noise ratio. We fitted the continuum with a model that includes a power law and the Galactic neutral hydrogen absorption and found this simple model is adequate in describing the overall broadband spectrum. For the observation #10498, we found a power law photon index of $\Gamma = 1.784 \pm 0.027$, and a 0.5 — 2 keV flux of 1.94×10^{-11} ergs cm^{-2}s^{-1} (see F10 for details). Unless otherwise noted, Errors are quoted at 90% confidence level throughout the paper.

3. MODELING

3.1. *Intrinsic Absorption*

In Figure 1 left panel we plot the X-ray spectrum of H 2356-309 between 1 and 40 Å for the observation

---

[3] see http://asc.havard.edu/ciao
[4] see http://asc.havard.edu/caldb
[5] see http://cxc.harvard.edu/contrib/letg/GainFilter/software.html.

#10498, in the observer's frame. In the right panel we show the enlarged portion between 21 and 22.5Å. An absorption feature is prominently located at ~ 22.05 Å. In the inset we show the stacked spectrum of the remaining nine *Chandra* observations, and indicate the wavelength of this feature, which was not detected, with a green arrow. In this inset the absorption feature seen at ~ 22.3 Å is an O VII Kα absorption line produced by the WHIM gas in the Sculptor Wall (see B09 and F10). There is no known instrumental feature near this feature (*Chandra* Proposers' Observatory Guide, or POG[6]). We examined both plus and minus orders and this feature is present in both sides with similar strength. The total exposure time of this observation is ~ 77 ksec. We also checked the consistency by splitting the exposure into two 38 ksec exposures, and we found this feature is consistently present in both exposures. We also checked the background spectrum and did not find any anomaly at this location that may have caused such an absorption feature. Considering also the transient nature of this feature, we conclude that it is not instrumental in origin.

With the assumption that this feature is intrinsic to H 2356-309, we examine the possible ion species based on a combination of chemical abundance and line strength (the oscillator strength f). Giving the detected wavelength, and assuming a very generous velocity range ($\pm 30,000$ km s^{-1}), the likely line transitions are O VII K$_\beta$ at $\lambda_{rest} = 18.63$ Å, Ca XVIII at $\lambda_{rest} = 18.70$ Å, Ar XV at $\lambda_{rest} = 18.82$ Å, O VIII at $\lambda_{rest} = 18.97$ Å, and Ca XVII at $\lambda_{rest} = 19.56$ Å. Here we select ion species with $f > 0.1$ only. Considering that both calcium and argon are orders of magnitude less abundant than oxygen, and we did not detect the corresponding O VII K$_\alpha$ transition, the most likely candidate is an intrinsic O VIII K$_\alpha$ absorber in an outflow.

We fitted the spectrum of the sequence #10498 with a model that includes the following components: (1) Galactic neutral hydrogen absorption with a fixed column density of $N_H = 1.33 \times 10^{20}$ cm^{-2} (Dickey & Lockman 1990); (2) a power law; (3) the WHIM and Galactic O VII K$_\alpha$ absorption lines at 21.6 and 22.3 Å, respectively (B09 and F10); and (4) an intrinsic absorption line at ~ 22.05 Å. We fixed the component (3) - the Galactic and the WHIM absorption lines - at the values obtained in F10. We chose the Voigt-profile based model that was described in B09 and F10 to fit the absorption feature (4); however, the exact form of the absorption line model is not important here, as long as the model can provide an adequate description of this feature. We limited the redshift range of this feature to account for an outflow velocity within 10,000 km s^{-1}, since most observed outflows from AGNs have velocities in the range of a few hundred to a few thousand km s^{-1} (Crenshaw et al. 2003). We performed the fit by minimizing the C-statistic, which is identical to maximizing the Poisson likelihood function (Cash 1979), and yields less biased best-fitting parameters than the standard χ^2 implementation (see Humphrey et al. 2009 for details).

Figure 1 shows the #10498 spectrum (black) and the fitted model (red). The 22.05 Å line has an equivalent width (EW) of 70.5 ± 20.5 mÅ. We are not able to constrain the upper limit on the O VIII K$_\alpha$ column density, and obtain a best-fit value of 7.6×10^{17} cm^{-2}, with a lower limit of 6.1×10^{16} cm^{-2}. The absorption feature is at a redshift of $z = 0.163 \pm 0.001$ relative to the observer system. We also found a Doppler-b parameter of $278.8^{+584.8}_{-159.6}$ km s^{-1}. Thermal broadening can at most provide a b parameter of up to 100 km s^{-1} (for hot gas with temperatures up to a few 10^7 K), indicating velocity gradient along the sight line plays a significant role in line broadening. If let free, both the Galactic line at 21.6 Å and the WHIM line at 22.3 Å are statistically insignificant due to low photon counts. This is consistent with what we found in the other Chandra observations (see Figure 2 of F10): both lines are weak in each individual spectrum and can only be detected when all the observations are analyzed simultaneously.

An accurate measurement of the BL Lac redshift is necessary to determine the outflow velocity. Based on the measurement of the optical absorption lines produced by the interstellar medium in the host galaxy, Falomo (1991) determined the redshift of H 2356-309 is $z = 0.165 \pm 0.002$. We find the measured redshifted of the O VIII K$_\alpha$ absorption line is very consistent with that of H 2356-309, with an outflow velocity of at most 1500 km s^{-1}.

We used Monte-Carlo simulations to assess the significance of this transient line. We fitted the #10498 spectrum with a model that does not include the intrinsic line. When comparing with the fit that includes the intrinsic line, we found a decrease in the C-statistic of $\Delta C_{obs} = 21.3$. This intrinsic line was discovered when we studied the 21 to 22.5 Å spectral region of 12 observations (11 *Chandra* and one *XMM*-Newton). For the Monte-Carlo simulation in each trial we made 12 mock spectra in this spectral region to mimic the 12 observations. Specifically, each mock spectrum was made with the model obtained from the real observation (see F10 for model parameters) but without any intrinsic line, i.e., we used the same power law index, normalization, exposure time, and two absorption lines (the Galactic and the WHIM) for that observation. We then searched each mock spectrum between 21 and 22.5 Å to identify any negative feature that could give a decrease of ΔC equal or larger than ΔC_{obs}. We ran a total of 40,000 trials, and found for 38 trials, there is at least one mock spectrum with a change in ΔC that is equal to, or greater than what was observed. This indicates a detection significance of 3.3σ, or 99.9% confidence level, accounting for the number of "trials".

When evaluating the detection significance we also fixed the Galactic and the WHIM absorption lines at the values obtained in F10. In principle, the two line parameters should be determined by a joint fit of all the 12 observations. However, such joint fit in our Monte-Carlo simulation is extremely computationally intensive, and our estimate indicated that the change in ΔC is negligible. Therefore, we decided to fix these two line parameters in our calculation.

We reiterate that the 21—22.5 Å range is the appropriate wavelength region over which to perform the random trials to assess the statistical significance of the 22.05 Å line, because it was only from examining this limited wavelength range that, by chance, we discovered this
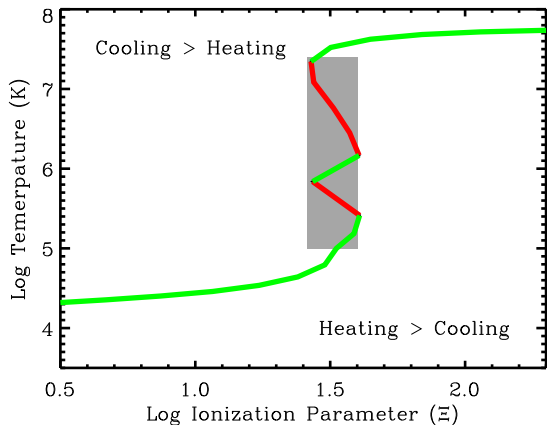
FIG. 2.— Thermal equilibrium curve. Green parts indicate stable states, while red parts indicate unstable states. The grey area shows the allowed region given by constraints on the ionization fractions.

transient line while studying the Sculptor WHIM in F10. However, for illustrative purposes only, we also computed the significance of this line by performing random trials over the entire 1—40 Å range and obtained a significance of 2.5σ, or 99.0% confidence. For comparison, it is worth noting that if we search the entire 1—40 Å range for other features in the 12 spectra, the strongest features we find are 5 candidate lines where the decrease in the C-statistic is greater than 10, with a maximum change of 15 ($\sim 1.7\sigma$). These candidates are even less significant than the 22.05 Å line and, importantly, none of them are associated with ion species (with strong oscillator strength) appropriate for the Milky Way, the blazar, or the Sculpor Wall WHIM absorber.

3.2. *Physical Properties*

Considering the redshift of the O VIII K_α absorption line, photonization by the central black hole of the blazar H 2356-309 likely plays a major role in ionizing the absorber. Therefore, we have used the photonization code CLOUDY to determine its physical condition. Calculations were performed with version 06.02 of CLOUDY, last described by Ferland et al. (1998).

In general, photo-ionized gas achieves thermal equilibrium by balancing heating with cooling, where the major heating source is the ionizing photons from the central black hole, and the major cooling mechanism is collisionally excited, atomic and ionic line emission. At high temperatures, heating by Compton scattering and cooling by thermal bremsstrahlung radiation and inverse Compton scattering will become important. Taking all these processes into consideration, we calculated the thermal equilibrium temperature as a function of the ionization parameter Ξ, using CLOUDY (see Figure 2). Following Krolik et al. (1981), this ionization parameter is defined as

$$\Xi \equiv \frac{L_i}{4\pi R^2 n_H c k T} \qquad (1)$$

where L_i is the luminosity of ionizing photons, R is the distance of the absorber to the central source, n_H is the gas density, k is the Boltzmann constant, and T is the gas temperature [7]. For simplicity, we adopted a power law spectrum with a photon index of $\Gamma = 1.784$, obtained from our *Chandra* spectrum, and also solar metallicity. We will discuss the impact of these choices later.

In Figure 2, cooling dominates over heating above the thermal equilibrium curve, and heating exceeds cooling below the curve. Along the equilibrium curve, the gas is thermally stable in the green parts, and unstable in the red parts where the gradient becomes negative. In the unstable states a small increase in temperature will lead to regions where heating exceeds cooling and therefore becomes unstable. The stable states include one "cold" ($T \leq 10^5$ K), one "hot" ($T > 10^7$ K), and one intermediate state ($T \sim 10^6$ K).

We also calculate the ionization fraction of both O VII and O VIII, following Krolik et al. (1985). The top panel of Figure 3 shows the ionization fraction of O VII (black line) and O VIII (red line) as a function of the ionization parameter Ξ; and the bottom panel of Figure 3 shows the ionization fraction as a function of temperature. We do not detect the intrinsic O VII K_α line, and estimate a 3σ upper limit of the line equivalent width of 24 mÅ. This puts a tight lower limit of $\Xi \gtrsim 25$, and $T \gtrsim 10^5$ K. On the other hand, the derived O VIII column density is about a few $\times 10^{17}$ cm^{-2}. It is therefore highly unlikely that the ionization fraction of O VIII is much smaller than 10^{-4} as this would imply a hydrogen column density much higher than 10^{24} cm^{-2} even for solar abundance. This puts a tight constraint on the upper limit of $\Xi \lesssim 40$, and $T \lesssim 2.5 \times 10^7$ K. Figure 2 shows this allowed region in grey.

The exact shape of the thermal equilibrium curve depends on assumptions such as the photon index of the incident spectrum and the metal abundance (see, e.g., Reynolds & Fabian 1995). A steeper spectrum (e.g., $\Gamma > 3$) will lower the Compton temperature at which Compton heating and cooling balance each other, therefore lowering the temperature of the "hot" stable state in Figure 2. On the other hand, a change in the metal abundance will also result in a change in the peak positions of the thermal equilibrium curve because of the metal line cooling mechanism. However, our estimates indicate unless these assumptions change dramatically, they do not have significant impact on the estimated parameters (ionization parameter, temperature, ionization fractions, etc.) here.

3.3. *Transient Nature of the Absorber*

The observation #10497 was taken immediately before this observation and ended on September 20th, 2008 at about 10AM; and the observation #10762 was taken immediately after this observation and started on September 25th, 2008 at about 2AM. This suggests the transient feature lasts at most $t_{max} \approx 4 \times 10^5$ seconds, and at least $t_{min} = 8 \times 10^4$ seconds.

---

[7] The other commonly used definition of the ionization parameter is $\xi \equiv \left(L_i / n_H R^2\right)$. The conversion between this two definitions (in c.g.s unit) is: $(\xi/\Xi) \approx 52\,T_6$, where T_6 is temperature in units of 10^6 K.
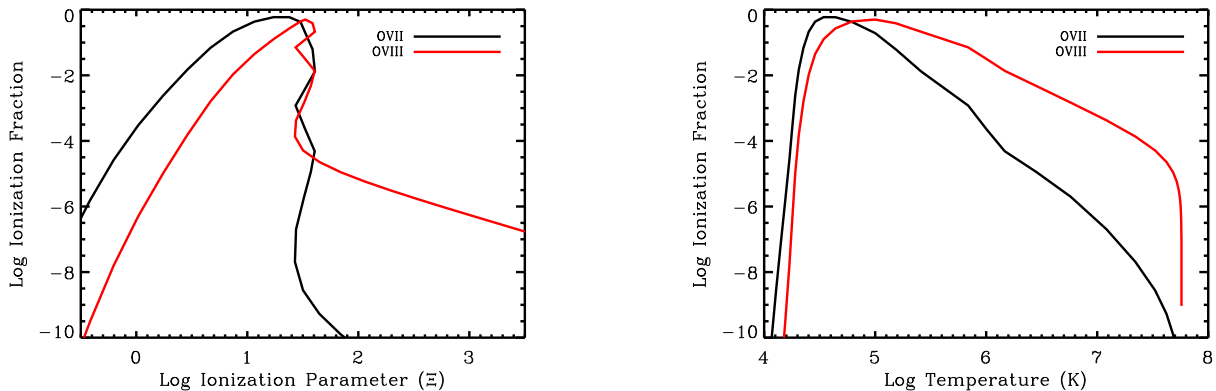
FIG. 3.— top panel: the ionization fraction of O VII (black line) and O VIII (red line) as a function of the ionization parameter Ξ; bottom panel: the ionization fraction of O VII (black line) and O VIII (red line) as a function of temperature.

Line variability is fairly common in the soft X-ray spectrum of AGNs. In particular, recent observations of AGNs with high resolution spectroscopy indicate narrow absorption lines can appear and vanish in time scales less than a few 100 ksec (e.g., Gibson et al. 2007). There are two likely scenarios that an absorption line can become transient: (1) the ionization structure of the absorber changes (see, e.g., Halpern 1984); or (2) the absorbing material changes, e.g., moving in and out of the sight line (see, e.g., Fabian et al. 1994). We consider both scenarios in the following discussion.

To change the physical state of the absorber during such a short period, either the ionizing source varies rapidly, or the absorber is in a physically unstable state. The source flux is extremely stable during our 500 ksec *Chandra* observations that span about four months (it varied at most about 30%; see F10). Furthermore, one *Chandra* and one *XMM*-Newton observation performed about one year before these *Chandra* observations showed variations about a factor of less than 2 (B09). Hence, the source variation is unlikely to be the cause of this transient feature.

Considering the possibility that the absorber becomes thermally unstable (the red parts in Figure 2), this intrinsic instability can lead to the transient nature of the absorber. In this case, the ionization structure can change rapidly if the photonization timescale is longer than the time interval t_{min}. This photonization timescale can be estimated as

$$t_{ion} = \left[\int_{\nu_{th}}^{\infty} \frac{L_\nu \sigma(\nu)}{4\pi R^2 h\nu} d\nu \right]^{-1}. \qquad (2)$$

Here L_ν ($\propto \nu^{-\alpha}$ where $\alpha = \Gamma - 1$ is the spectral index) is the ionizing photon flux, σ is the photonization cross section and $\propto (\nu_{th}/\nu)^3$, ν_{th} is the photonization threshold frequency, and h is the Planck constant. Adopting the numbers for O VIII (Verner et al. 1996), we found $t_{ion} \approx 2 \times 10^4 R_{pc}^2 L_{46}^{-1}$ s. Here R_{pc} is the distance to the absorber in units of pc, and L_{46} is the ionizing luminosity in units of 10^{46} ergs s^{-1}. For H 2356-309, L_i, the luminosity of the ionizing photons, is $\sim 5 \times 10^{45}$ ergs s^{-1}. If

$t_{ion} \gtrsim t_{min}$, we found the distance of the absorber must be $R \gtrsim 3$ pc. This distance would put the absorbing material somewhere between the typical broad line region (BLR, sub-pc) and narrow line region (NLR, 10 pc – 1 kpc) of an AGN. The density of the absorber then is

$$n_H \approx 7 \times 10^5 R_{pc}^{-2} T_6^{-1} \Xi_{30}^{-1} L_{46} \text{ cm}^{-3}, \qquad (3)$$

where T_6 is the temperature in units of 10^6 K, and Ξ_{30} is the ionization parameter in units of 30. Taking the typical values for H 2356-309, the density is $n_H \approx 4 \times 10^5$ cm^{-3}. With this density, the typical recombination time scale, $t_{rec} \approx 4 \times 10^6$ $T_6^{1/2} (n_H/10^5 \text{ cm}^{-3})^{-1} \approx 10^7$ seconds , is also longer than t_{min}.

If instead the absorber is stable but moves in and out of the sight line between observations, then all the time scales must be shorter than t_{max}. The absorber then has an upper limit on the distance of $R \lesssim 6$ pc (from $t_{ion} < t_{max}$), and a lower limit on the density of $n_H \gtrsim 10^6$ cm^{-3} (from $t_{rec} < t_{max}$). The O VIII column density is $\sim 10^{17}$ cm^2. Assuming solar metallicity and an ionization fraction of 0.5, the size of the absorber along the sight line is $\sim 3 \times 10^{13}$ cm. If the absorber has a similar size in the perpendicular direction, it implies a light crossing time of $\sim 3 \times 10^5$ seconds if the velocity in that direction is $\sim 1,000$ km s^{-1}. Since this time is less than t_{max}, this scenario is also consistent with the data.

We can also estimate the mass loss rate assuming a uniform spherically symmetric outflow (Krolik et al. 1985):

$$\dot{M} = f \frac{m_H \upsilon L_i}{ckT\Xi}$$
$$\approx 15 f_{0.1} \ L_{45} T_6^{-1} \upsilon_{1000} \Xi_{30}^{-1} \text{ M}_\odot \text{yr}^{-1}, \qquad (4)$$

Here m_H is the hydrogen mass, υ_{1000} is the outflow velocity in units of 1,000 km s^{-1}, and f is the covering fraction and is roughly 0.1 — the fraction of observational time showing the line. This value is higher than those of Seyfert galaxies which typically have weak outflows (~ 1M$_\odot$yr^{-1}, e.g., Steenbrugge et al. 2005), but comparable to those AGNs with energetic jets (e.g., Sternberg & Soker 2009). The mass loss rate is likely smaller if it is
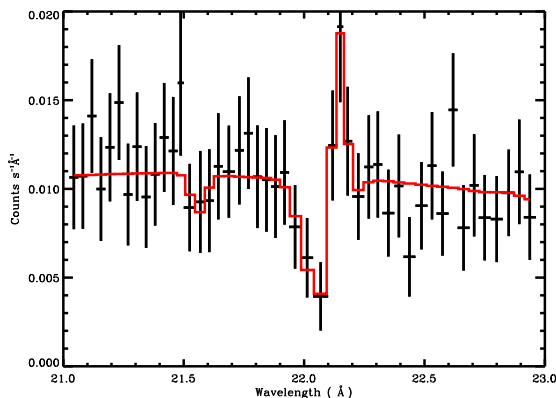
FIG. 4.— Spectral fitting with a P Cygni-type profile, which includes one absorption line model on the short-wavelength side, and one emission line on the long-wavelength side. The wavelength is plotted in the obseverber's frame.

beamed. Such a radial outflow can produce a P Cygni-type line profile typically seen in a stellar wind (Krolik et al. 1985). Interestingly, we do obtain a marginal detection of an emission feature on the long-wavelength side of the absorption feature, as expected from the P Cygni profile (see discussion below.)

4. DISCUSSION

4.1. A Possible P Cygni Profile?

The P Cygni-type of line profile was originally discovered in the optical and ultraviolet spectra of stellar objects, and is often attributed to the stellar wind (e.g., Lamers et al. 1987). With *Chandra*, the X-ray P Cygni line was first detected in the spectrum of Circinus X-1, a Galactic X-ray binary (Brandt & Schulz 2000; Schulz & Brandt 2002) and, subsequently, it was also found in the X-ray spectra of active galactic nuclei (e.g, Kaspi et al. 2001). A P Cygni-type of line profile provides an important diagnostic tool of whether the outflow is beamed with a jet-like structure or is more spherically extended.

In the observation #10498, we find a possible emission feature right next to the absorption feature on the long-wavelength side, resembling a P Cygni-type profile. We fit this emission feature with a Gaussian profile, along with an absorption profile on the short-wavelength side (see Figure 4, plotted in the observer's frame). We find this is sufficient for fitting the absorption-emission feature at 22.05 Å. Using Monte-Carlo simulations as described in § 3.1, we found this feature is detected at the 2.3σ level. If this transient emission feature is O VIII $K\alpha$ and can be associated with the absorber, we measured an O VIII line flux of 8.2×10^{-5} photons cm^{-2}s^{-1}. The O VIII line emissivity peaks at about 3×10^6 K. Assuming a peak emissivity, we obtained an upper limit of the emission measure of $EM = \int n_e^2 dV \approx 5 \times 10^{10}$ cm^{-6}pc^3 at the distance of the BL Lac. Here n_e is the electron density and the integration is over the emission volume. However, we consider the P Cygni scenario unlikely since if the $n_e \sim 10^6$ cm^{-3} as we estimated for the absorber, the linear size of the emission material (~ 0.4 pc) would

be far greater than that of the absorber. Clearly, more sophisticated modeling is necessary to fully understand the structure and physical properties of this material as revealed by the emission/absorption profile.

4.2. Host galaxy, Intervening or Local Absorption?

The transient nature of this absorption feature makes it very unlikely to be produced by the ISM in the host galaxy, an intervening absorber, or a local absorber. We do notice that the observed wavelength of this feather is very close to the rest wavelength of the O VI K_α inner shell transition ($\lambda = 22.02$ Å, see Pradhan et al. 2003; Schmidt et al. 2004). This O VI K_α inner shell transition was first reported in Lee et al. (2001) in the X-ray spectrum of MCG-6-30-15.

4.3. Summary

X-ray observations of narrow absorption features offer a unique opportunity to probe the inner region of BL Lac objects. In this paper we report the detection of a transient absorption line during our H 2356-309 campaign with the *Chandra* X-ray Telescope. This line is most likely produced by O VIII in a photo-ionized outflow intrinsic to the BL Lac object H 2356-309. Considering the transient nature of the absorber, we obtain constrains on the absorber's ionization parameter, $25 \lesssim \Xi \lesssim 40$, temperature, $10^5 < T < 2.5 \times 10^7$ K, and density, a few $\times 10^5$ cm^{-3}.

Our detection is quite different from X-ray absorption features detected in BL Lac objects before *Chandra* and *XMM*-Newton (e.g., Canizares & Kruper 1984; Madejski et al. 1991). Those absorption features typically have a velocity width of up to a few $\times 10^4$ km s^{-1}, while in H 2356-309, the velocity is at most $1 - 2 \times 10^3$ km s^{-1}. However, even in our case, the line width is much larger than that expected from thermal broadening, suggesting an outflow as a likely cause of the broadening.

Blustin et al. (2004) studied the *XMM*-Newton RGS spectra of four BL Lac objects with previously known, broad X-ray absorption lines and found none. Perlman et al. (2005) also analyzed the X-ray spectra of 13 bright BL Lac objects observed with *XMM*-Newton. They did not detect any broad, intrinsic features either, but they found strong evidence for the intrinsic curvature of the spectral index of most of the targets. In both studies, they concluded that the previously reported features were due to a combination of calibration uncertainties and the use of a overly simplified, single power-law model. At low resolution and low S/N a spectral curvature can mimic a broad absorption if the spectrum was fitted with a single power law (Perlman et al. 2005). However, our observation, which has none of these problems, along with their detections of several unexplainable absorption features detected in Blustin et al. (2004), raise again the question of whether or not such absorption is common in BL Lac objects. The high variability of the BL Lac object and its environment make it a challenge to address this issue. We detect this line in one (~ 80 ksec) observation for a total of 12 (~ 600 ksec for *Chandra*, and ~ 130 ksec for *XMM*-Newton) observations. Taking this probability at face value, a long-term, monitoring program which focuses on several bright BL Lac objects would be a

feasible approach to unveil the nature of these transient absorption lines.

REFERENCES

Angel, J. R. P., & Stockman, H. S. 1980, ARA&A, 18, 321

Brandt, W. N., & Schulz, N. S. 2000, ApJ, 544, L123

Blustin, A. J., Page, M. J., & Branduardi-Raymont, G. 2004, A&A, 417, 61

Buote, D. A., Zappacosta, L., Fang, T., Humphrey, P. J., Gastaldello, F., & Tagliaferri, G. 2009, ApJ, 695, 1351

Canizares, C. R., & Kruper, J. 1984, ApJ, 278, L99

Cash, W. 1979, ApJ, 228, 939

Crenshaw, D. M., Kraemer, S. B., & George, I. M. 2003, ARA&A, 41, 117

Dickey, J. M., & Lockman, F. J. 1990, ARA&A, 28, 215

Fabian, A. C., et al. 1994, PASJ, 46, L59

Falomo, R. 1991, AJ, 101, 821

Fang, T., Marshall, H. L., Lee, J. C., Davis, D. S., & Canizares, C. R. 2002, ApJ, 572, L127

Fang, T., Sembach, K. R., & Canizares, C. R. 2003, ApJ, 586, L49

Fang, T., Buote, D. A., Humphrey, P. J., Canizares, C. R., Zappacosta, L., Maiolino, R., Tagliaferri, G., & Gastaldello, F. 2010, arXiv:1001.3692

Ferland, G. J., Korista, K. T., Verner, D. A., Ferguson, J. W., Kingdon, J. B., & Verner, E. M. 1998, PASP, 110, 761

Gibson, R. R., Canizares, C. R., Marshall, H. L., Young, A. J., & Lee, J. C. 2007, ApJ, 655, 749

Grandi, P., et al. 1997, A&A, 325, L17

Halpern, J. P. 1984, ApJ, 281, 90

HESS Collaboration, et al. 2010, arXiv:1004.2089

Humphrey, P. J., Liu, W., & Buote, D. A. 2009, ApJ, 693, 822

Kaspi, S., et al. 2001, ApJ, 554, 216

Krolik, J. H., McKee, C. F., & Tarter, C. B. 1981, ApJ, 249, 422

Krolik, J. H., Kallman, T. R., Fabian, A. C., & Rees, M. J. 1985, ApJ, 295, 104

Lamers, H. J. G. L. M., Cerruti-Sola, M., & Perinotto, M. 1987, ApJ, 314, 726

Lee, J. C., Ogle, P. M., Canizares, C. R., Marshall, H. L., Schulz, N. S., Morales, R., Fabian, A. C., & Iwasawa, K. 2001, ApJ, 554, L13

Madejski, G. M., Mushotzky, R. F., Weaver, K. A., Arnaud, K. A., & Urry, C. M. 1991, ApJ, 370, 198

Nicastro, F., et al. 2002, ApJ, 573, 157

Nicastro, F., et al. 2005, ApJ, 629, 700

Nicastro, F., et al. 2005, Nature, 433, 495

Perlman, E. S., et al. 2005, ApJ, 625, 727

Plotkin, R. M., et al. 2010, AJ, 139, 390

Pradhan, A. K., Chen, G. X., Delahaye, F., Nahar, S. N., & Oelgoetz, J. 2003, MNRAS, 341, 1268

Rasmussen, A., Kahn, S. M., & Paerels, F. 2003, The IGM/Galaxy Connection. The Distribution of Baryons at z=0, 281, 109

Reynolds, C. S., & Fabian, A. C. 1995, MNRAS, 273, 1167

Urry, C. M., Mushotzky, R. F., & Holt, S. S. 1986, ApJ, 305, 369

Sambruna, R. M., George, I. M., Madejski, G., Urry, C. M., Turner, T. J., Weaver, K. A., Maraschi, L., & Treves, A. 1997, ApJ, 483, 774

Sbarufatti, B., Treves, A., Falomo, R., Heidt, J., Kotilainen, J., & Scarpa, R. 2005, AJ, 129, 559

Schmidt, M., Beiersdorfer, P., Chen, H., Thorn, D. B., Träbert, E., & Behar, E. 2004, ApJ, 604, 562

Schulz, N. S., & Brandt, W. N. 2002, ApJ, 572, 971

Steenbrugge, K. C., et al. 2005, A&A, 434, 569

Sternberg, A., & Soker, N. 2009, MNRAS, 398, 422

Urry, C. M., & Padovani, P. 1995, PASP, 107, 803

Verner, D. A., Ferland, G. J., Korista, K. T., & Yakovlev, D. G. 1996, ApJ, 465, 487

Williams, R. J., et al. 2005, ApJ, 631, 856